

Supplementary Materials: Molecular Dynamics Investigation of Phenolic Oxidative Coupling Protein Hyp-1 Derived from *Hypericum perforatum*

Joanna Smietanska *, Tomasz Kozik, Radoslaw Strzalka, Ireneusz Buganski and Janusz Wolny

Faculty of Physics and Applied Computer Science, AGH University of Science and Technology, Krakow, 30-962, Poland; tomasz.kozik@fis.agh.edu.pl (T.K.); strzalka@fis.agh.edu.pl (R.S.); buganski@fis.agh.edu.pl (I.B.); wolny@fis.agh.edu.pl (J.W.)

* Correspondence: joanna.smietanska@fis.agh.edu.pl

Supplementary Materials

Table S1. Overall comparison of the rotamer outliers within Hyp-1 structure. Values in the second column refer to the torsion values in the refined Hyp-1 model with respect to the separate chains A/B. Ranges of the most populated simulated dihedral angles were placed in the third column. Their percentage probability values within the 40° x 40° region are labeled in the fourth column, while the suggested rotamer is mentioned in last column.

Residue	Refined A/B torsion angles	Range of most populated torsion angles (°)	Probability of χ_1 or $\chi_1\chi_2$ combination within region (%)	Suggested rotamer
Pro16	25/18 (endo 44%) ^a	0–40, 320–360	62	endo 44%/ exo 43%
Pro64	352/344 (exo 43%)	0–40	87	endo 44%
Pro122	335/350 (exo 43%)	0–40	100	endo 44%
Pro124	333/337 (exo 43%)	0–40	82	endo 44%
Ser112	297/294 (m 29%)	0–40	41	p 48%
Val7	173/177 (t 73%)	160–200	40	t
Val24	174/174 (t 73%)	280–320	72	p 48%
Val30	177/169 (t 73%)	280–320	70	p 48%
Val32	176/173 (t 73%)	280–320	76	p 48%
Val38	176/176 (t 73%)	280–320	95	p 48%
Val51	160/171 (t 73%)	280–320	98	p 48%
Val54	173/174 (t 73%)	280–320	99	p 48%
Val60	298/296 (m 20%)	160–200	45	t
Val99	185/185 (t 73%)	160–200	30	t
Val100	172/178 (t 73%)	280–320	97	p 48%
Val103	174/172 (t 73%)	280–320	99	p 48%
Val108	179/174 (t 73%)	40–80	81	m
Val118	185/183 (t 73%)	280–320	100	p 48%
Val128	177/179 (t 73%)	280–320	99	p 48%
Val133	165/175 (t 73%)	280–320	88	p 48%
Val147	166/170 (t 73%)	280–320	100	p 48%
Val157	170/175 (t 73%)	280–320	98	p 48%
Thr5	295/298 (m 43%)	40–80	52	p
Thr53	294/291 (m 43%)	160–200	45	t
Thr55	58/58 (p 49%)	280–320	99	m
Thr66	297/57 (m 43%/ p 49%)	280–320	95	m
Thr85	297/295 (m 43%)	40–80	98	p
Thr117	74/300 (p 49%/295)	40–80	99	p
Thr119	299/298 (m 43%)	40–80	100	p
Thr127	186/194 (t 7%)	40–80	100	p
Leu86	168/170, 65/60 (tp 29%)	160–200, 160–200	76	tt
Leu151	294/295, 174/176 (mt 59%)	280–320, 280–320	82	mt
Phe72	290/291, 337/347 (m-30 9%)	280–320, 280–320	85	m-85

Phe158	302/304, 318/327 (m-30 9%)	280–320, 280–320	83	m-85
His63	194/196, 285/286 (t-80 11%)	160–200, 240–280	79	t-80
His70	290/289, 274/279 (t-80 11%)	280–320, 160–200	75	m170
Asp94	288/293, 321/308 (m-20 51%)	160–200, 0–40	47	t0
Asn95	58/59, 314/313 (p-10 7%)	40–80, 80–120	77	p30
Asn154	298/304, 273/275 (m-80 8%)	280–320, 80–120	80	m120

^a Values in parentheses correspond to the reference rotamer from the Penultimate Library and its population.

Table S2

Residue	Refined A/B torsion angles	Range of most populated torsion angles (°)	Suggested rotamer
Glu102	297/185, 181/158, 259/52 (mt-10 33%/tt0 24%) ^a	160–200, 280–320, 0–40	tm-20
Glu106	60/296, 181/146, 66/33 (pt-20 5%/ mt-10 33%)	160–200, 40–80, 0–40	tp10
Glu130	289/189, 160/165, 17/14 (mt-10 33%/tt0 24%)	160–200, 40–80, 0–40	tp10
Glu132	282/303, 187/172, 335/59 (mt-10 33%)	160–200, 40–80, 0–40	tp10
Glu142	276/287, 157/174, 15/358 (mt-10 33%)	80–120, 160–200, 120–160	pt-20
Glu149	298/170, 179/180, 46/21 (mt-10 33%/tt0 24%)	120–160, 280–320, 0–40	-
Gln35	293/298, 209/183, 294/18 (mt-30 35%)	280–320, 160–200, 40–80	mt-30
Gln146	291/282, 174/189, 39/270 (mt-30 35%)	240–280, 280–320, 320–360	mm-40
Met1	294/177, 187/192, 308/294 (mtm11%/ttm 7%)	280–320, 160–200, 80–120	mtp
Met68	301/298, 175/184, 285/285 (mtm11%)	280–320, 160–200, 160–200	mtt
Lys8	321/299, 248/281, 206/283, 190/91 (mmtt 6%/mmtt 1%)	280–320, 120–160, 80–120, 160–200	mtpt
Lys21	288/176, 189/137, 201/190, 136/217 (mttt 20%/tttt 13%)	280–320, 160–200, 160–200, 160–200	mttt
Lys33	295/189, 192/173, 196/187, 297/323 (mttm 5%/tttm 3%)	280–320, 160–200, 160–200, 160–200	mttt
Lys40	180/75, 166/172, 66/165, 171/172 (ttpt 2%/pttt 2%)	160–200, 160–200, 160–200, 160–200	tttt
Lys83	179/176, 184/174, 164/281, 279/177 (tttm 3%/ttmt 2%)	160–200, 200–240, 80–120, 160–200	tttt
Lys113	185/67, 222/163, 78/100, 147/85 (ttpt 2%/pttp 1%)	160–200, 160–200, 160–200, 160–200	tttt
Lys138	156/210, 203/198, 153/178, 76/201 (tttp 4%/tttt 13%)	160–200, 160–200, 80–120, 160–200	tttt
Lys145	297/297, 302/300, 280/295, 187/185 (mmtt 1%)	280–320, 280–320, 160–200, 160–200	mmtt
Arg27	196/67, 235/183, 260/288, 103/286 (ttm105 1%/ ptm-85 1%)	160–200, 160–200, 40–80, 240–280	ttp-105
Arg93	310/299, 204/201, 78/286, 169/178 (mtp180 5%/mtm180 5%)	280–320, 160–200, 40–80, 160–200	mtp180

^a Values in parentheses correspond to the reference rotamer from the Penultimate Library and its population.

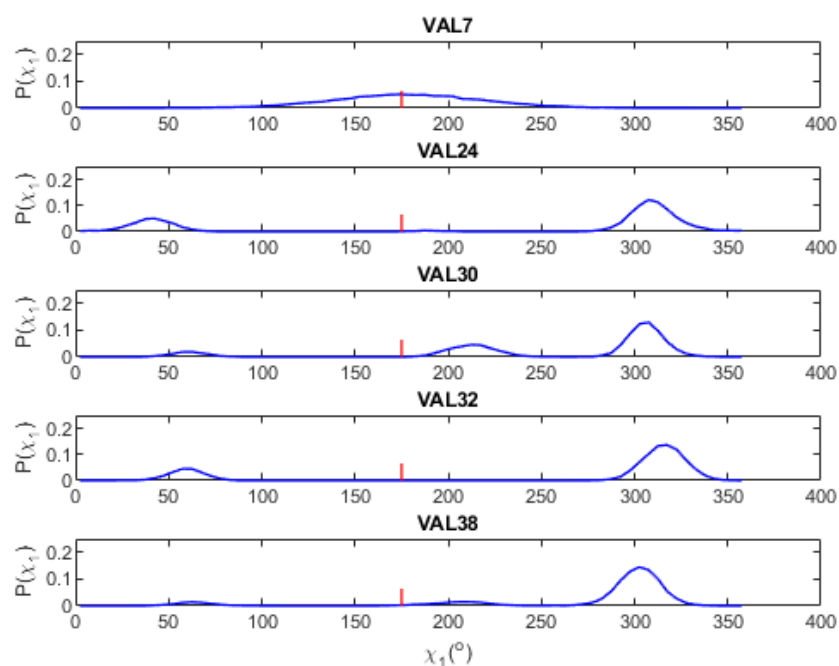


Figure S1. Side chain torsions probability density distributions $P(\chi_1)$ (solid blue lines) for Val7, Val24, Val30, Val32 and Val38. Values of χ_1 angles observed in the refined Hyp-1 model were marked as solid red lines.

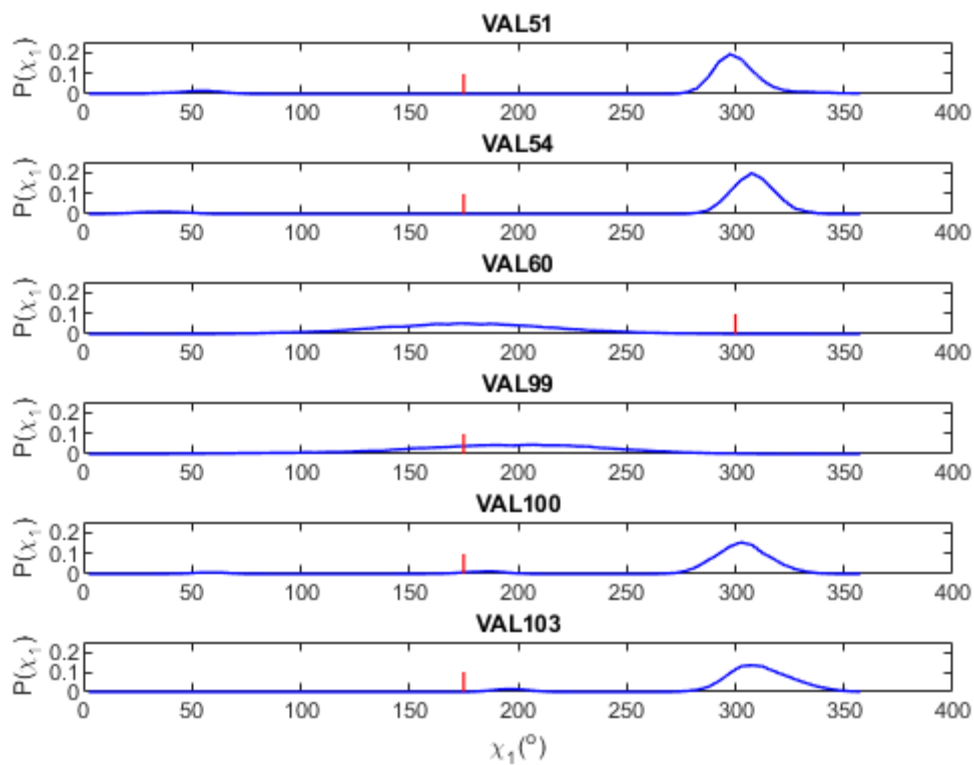


Figure S2. Side chain torsions probability density distributions $P(\chi_1)$ (solid blue lines) for Val51, Val54, Val60, Val99, Val100 and Val103. Values of χ_1 angles observed in the refined Hyp-1 model were marked as solid red lines.

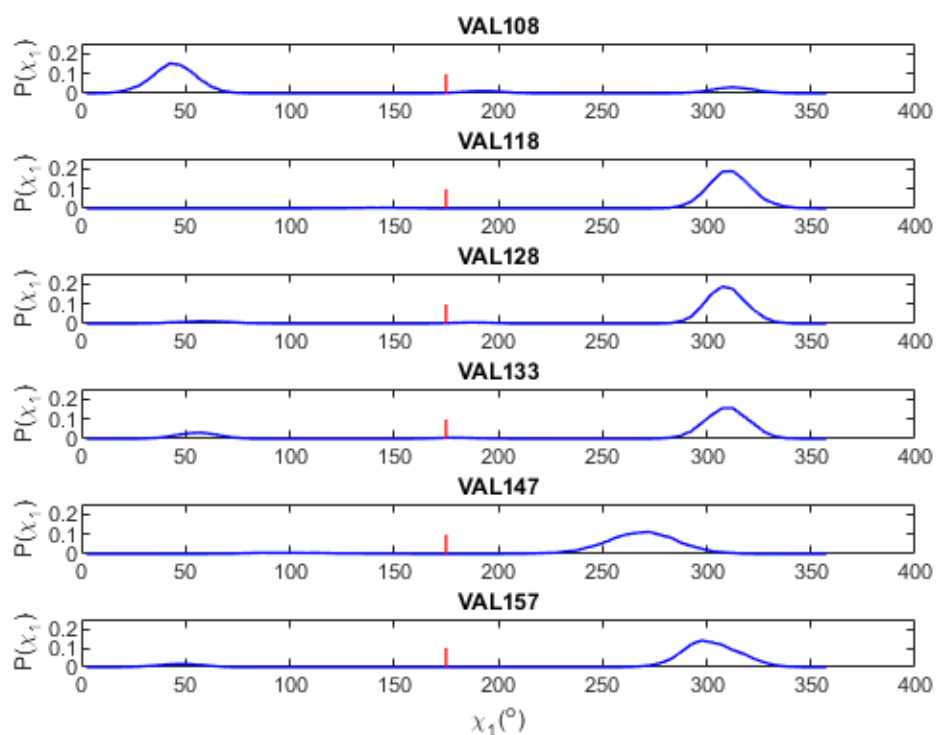


Figure S3. Side chain torsions probability density distributions $P(\chi_1)$ (solid blue lines) for Val108, Val118, Val128, Val133, Val147 and Val157. Values of the χ_1 angles observed in the refined Hyp-1 model were marked as solid red lines.

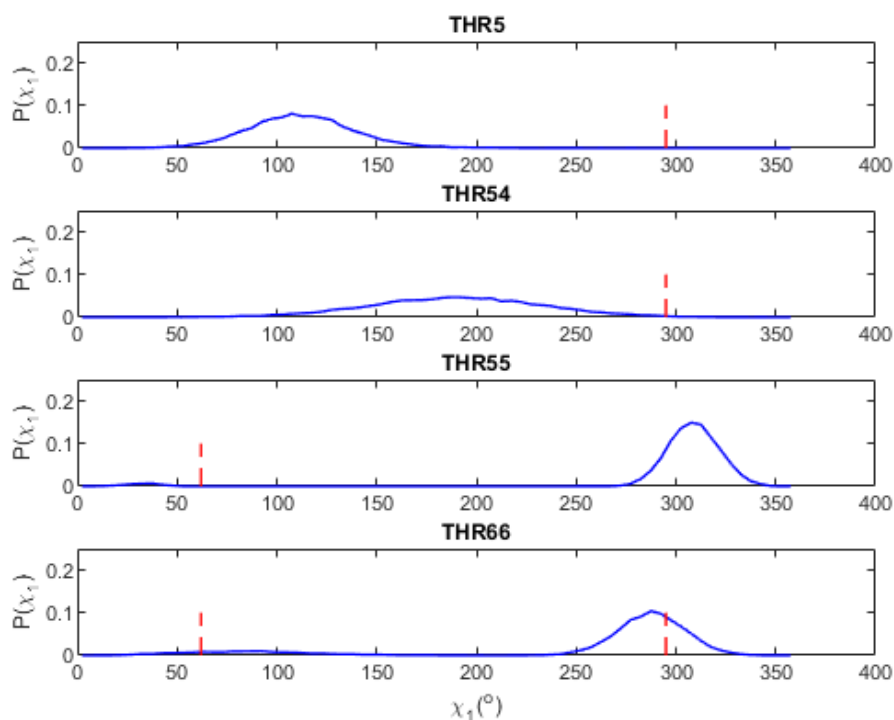


Figure S4. Side chain torsions probability density distributions $P(\chi_1)$ (solid blue lines) for Thr5, Thr54, Thr55 and Thr66. Values of the χ_1 angles observed in the refined Hyp-1 model were marked as red dashed lines.

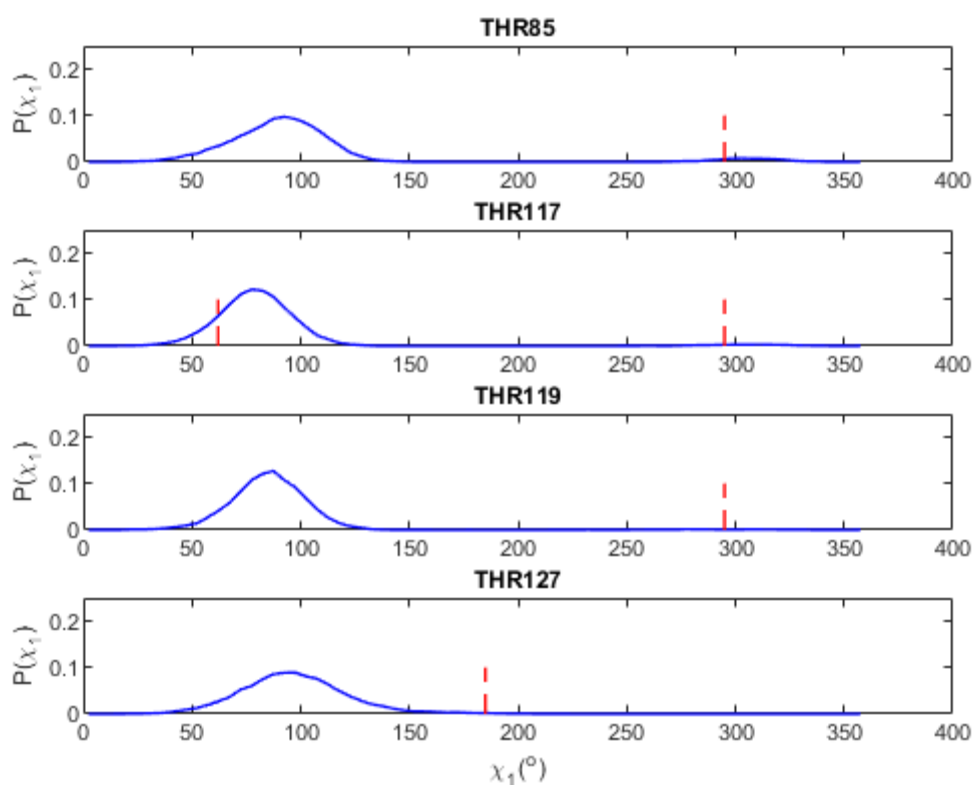


Figure S5. Side chain torsions probability density distributions $P(\chi_1)$ (solid blue lines) for Thr85, Thr117, Thr119 and Thr127. Values of the χ_1 angles observed in the refined Hyp-1 model were marked as red dashed lines.

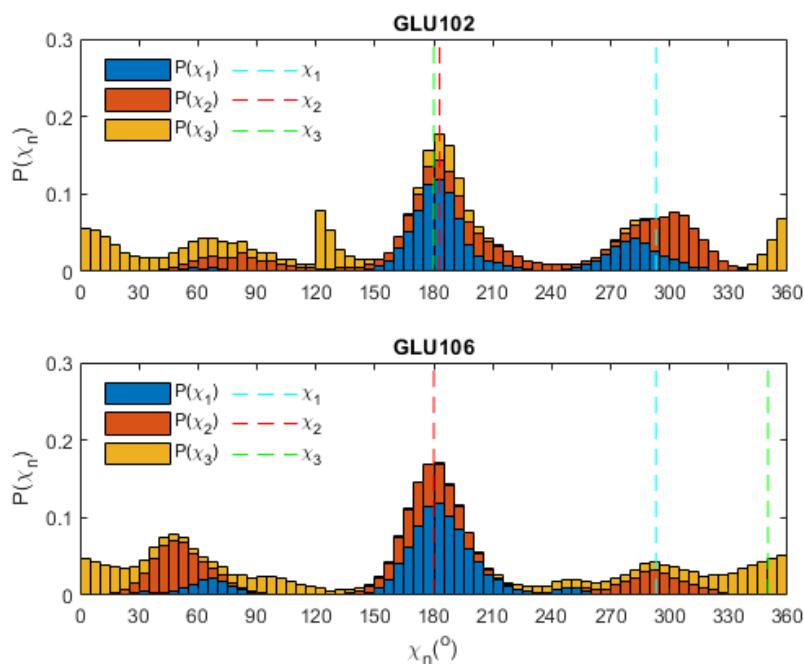


Figure S6. Stacked bar graph of the side chain χ_1 , χ_2 , χ_3 torsions probability distributions for Glu102 and Glu106. The probability values within $5^\circ \times 5^\circ$ bins for separate torsion angles were marked as blue, orange and yellow, respectively. Appropriate values of the χ_1 , χ_2 , χ_3 angles from the refined Hyp-1 model were presented sequentially as light blue, red and light green dashed lines.

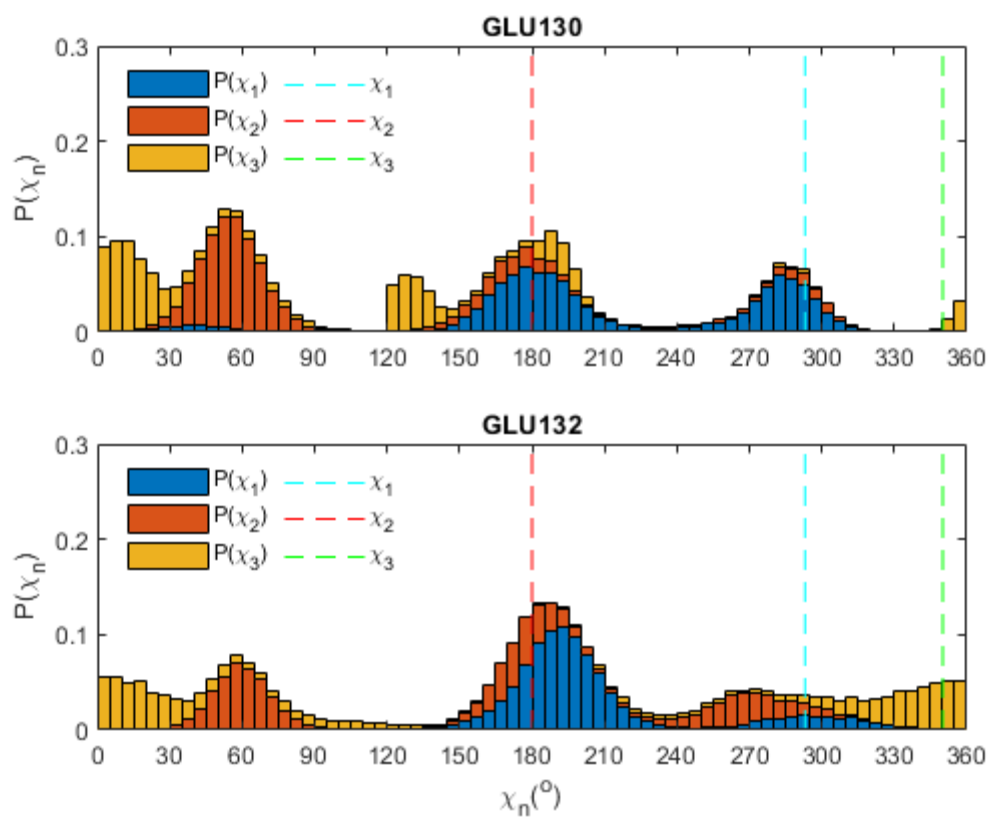


Figure S7. Stacked bar graph of the side chain χ_1 , χ_2 , χ_3 torsions probability distributions for Glu130 and Glu132. The probability values within $5^{\circ} \times 5^{\circ}$ bins for separate torsion angles were marked as blue, orange and yellow, respectively. Appropriate values of χ_1 , χ_2 , χ_3 angles from the refined Hyp-1 model were presented sequentially as light blue, red and light green dashed lines.

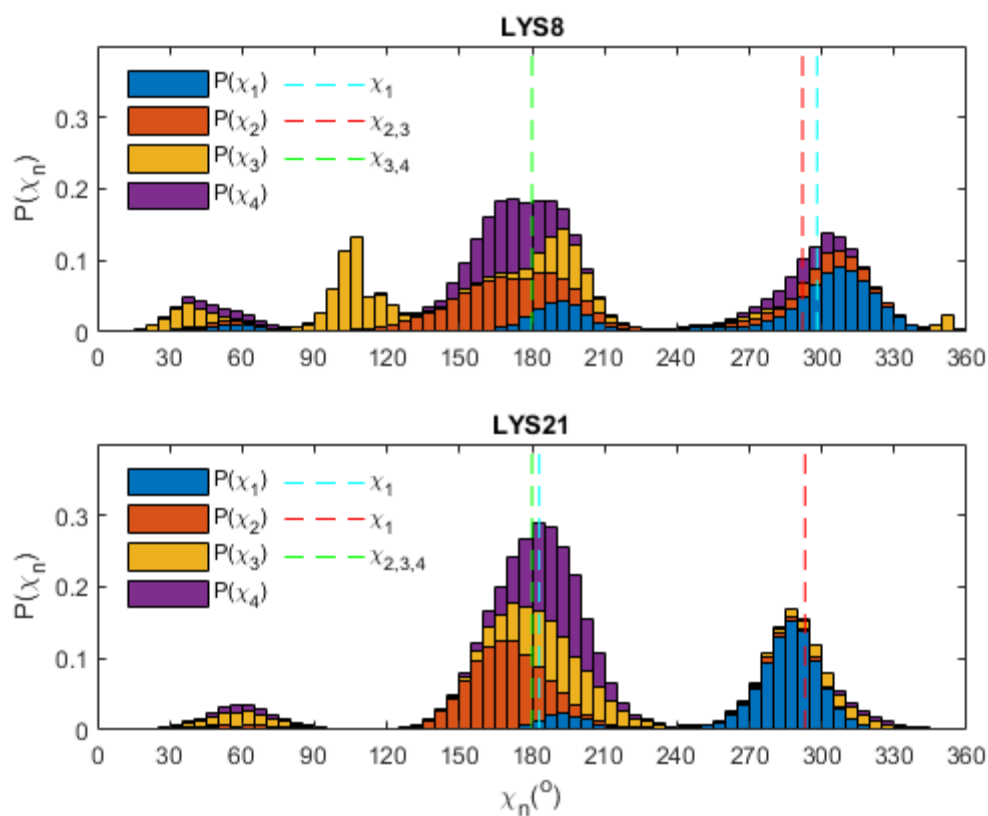


Figure S8. Stacked bar graph of the side chain χ_1 , χ_2 , χ_3 , χ_4 torsions probability distributions for Lys8 and Lys21. The probability values within $5^{\circ} \times 5^{\circ}$ bins for separate torsion angles were marked as blue, orange, yellow and purple, respectively. Appropriate values of χ_1 , χ_2 , χ_3 angles from refined Hyp-1 model were presented sequentially as light blue, orange and light green dashed lines. If one χ value is common for multiple torsion angles in the side chain, we marked them as a single line with a proper index to prevent line overlap and confusion during the figure interpretation.

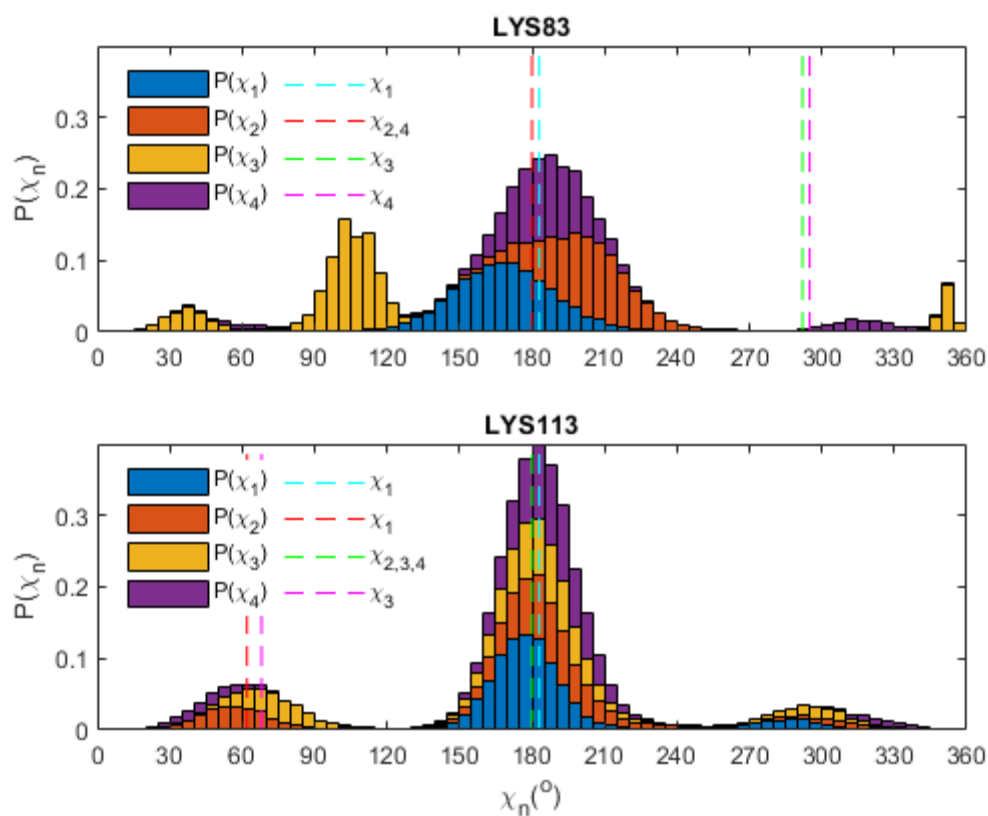


Figure S9. Stacked bar graph of the side chain χ_1 , χ_2 , χ_3 , χ_4 torsions probability distributions for Lys83 and Lys113. The probability values within $5^{\circ} \times 5^{\circ}$ bins for separate torsion angles were marked as blue, orange, yellow and purple, respectively. Appropriate values of χ_1 , χ_2 , χ_3 angles from refined Hyp-1 model were presented sequentially as light blue, orange and light green dashed lines. If one χ value is common for multiple torsion angles in the side chain, we marked them as a single line with a proper index to prevent line overlap and confusion during figure interpretation.

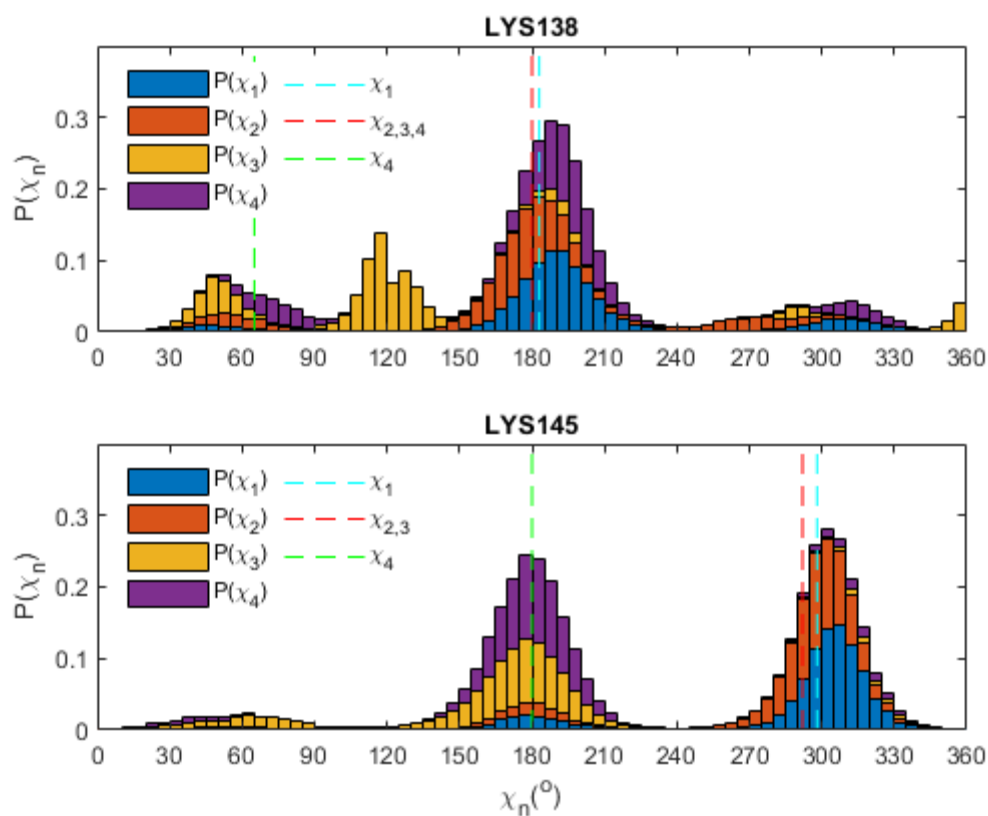


Figure S10. Stacked bar graph of the side chain χ_1 , χ_2 , χ_3 , χ_4 torsions probability distributions for Lys138 and Lys145. The probability values within the $5^{\circ} \times 5^{\circ}$ bins for separate torsion angles were marked as blue, orange, yellow and purple, respectively. Appropriate values of χ_1 , χ_2 , χ_3 angles from the refined Hyp-1 model were presented sequentially as light blue, orange and light green dashed lines. If one χ value is common for multiple torsion angles in the side chain, we marked them as a single line with a proper index to prevent line overlap and confusion during figure interpretation.